

# Identifying the Suitability of Environmental Friendly Fe<sub>2</sub>O<sub>3</sub> Nanomaterials for Supercapacitor Applications

Priyadharshini Muthukumaravel<sup>\*1</sup>, Rajesh Pattulingam<sup>1</sup>, Syed Illiyas Syed Maqbool<sup>1</sup>, Hariharan Venkatesan<sup>2</sup> and Ezhil Inban Manimaran<sup>3</sup>

<sup>1</sup>Department of Chemistry, Government Arts College, Coimbatore-641018, Tamilnadu, India.

<sup>2</sup>Department of Physics, Mahendra Arts and Science College, Namakkal-637501, Tamilnadu, India.

<sup>3</sup>Department of Physics, Government Arts College, Coimbatore-641018, Tamilnadu, India.

## ARTICLE INFO

### Article history:

Received: 9 July 2021;

Received in revised form:

1 August 2021;

Accepted: 10 August 2021;

### Keywords

Nanoparticles,  
Electrochemical,  
Supercapacitor,  
Charge Density.

## ABSTRACT

Environmental friendly  $\alpha$ -Fe<sub>2</sub>O<sub>3</sub> nanoparticles were successfully synthesized via a facile and cost effective chemical precipitation method with the extraction of *Nyctanthesarbortristis* for the first time. Also it is undergone at room temperature for super capacitor applications and that was observed through electrochemical studies. The prepared samples were characterized by powder X-ray diffraction (XRD), Field emission Scanning electron microscopy (FE-SEM) and UV visible spectroscopic studies. The powder X-ray diffraction study revealed the formation of  $\alpha$ -Fe<sub>2</sub>O<sub>3</sub> in the case of annealed sample. Microscopic images displays that the  $\alpha$ -Fe<sub>2</sub>O<sub>3</sub> nanoparticles were highly agglomerated in nature with the dimension of the order of 2-3  $\mu$ m. Cyclic voltammetry and simultaneous galvanostatic charge/discharge studies were performed in order to find out the suitability of the material for Supercapacitor applications. The electrochemical results explores that the annealed sample ( $\alpha$ -Fe<sub>2</sub>O<sub>3</sub>) had improved performance due to its structural with superiority nature. Moreover, the capacitance retention of the  $\alpha$ -Fe<sub>2</sub>O<sub>3</sub> based electrode shows highly stable performance and also its suitability as a lasting electrode material for Super capacitor applications.

© 2021 Elixir All rights reserved.

## Introduction

In recent years, the global importance of semiconducting metal oxides in the various fields of science and technology that continuously paid more attention in the study and the development of various synthesis methods for corresponding applications. Moreover, metal oxide based semiconducting nano materials have become a rapidly emerging new field in materials science which covers both chemistry and physics [1]. In this regard earlier reports using literature support the suitability of Iron Oxide based nano materials for bio sensor applications in particular green synthesized metal oxide based nano dimensional materials. Sardar et.al prepared Iron Oxide nanomaterials by using green synthesis approach in association with Gooseberry leaves and that acted as a reducing agent during synthesis process. These observations suggested that electrochemical behavior of Iron oxide nanomaterials may be a promising candidate for bio sensing applications and showed enhanced efficiency of the prepared materials [2]. Urbanova et.al., completely reviewed about the sensing properties of Iron Oxide nanoparticles in detail and discusses about the properties of enzymatic sensors in detail [3]. On the other hand, various metal oxides were also analyzed in order to find their suitability for bio sensor applications. For example, Nirmalya et.al, analyzed the unique properties of ZnO nanoparticles in association with different metal oxides for bio sensor applications. In addition with the above, they have also discussed the future aspects of nano hybrid materials for sensor applications [4]. Mathias et.al., dealt high refractive index dielectric materials in order to increase the sensitivity factor of a gold thin film despite its

large evanescent electromagnetic field decay lengths. Hence, Iron oxide nanoparticles were grafted onto a gold thin film and were easily functionalized by biomolecular receptors through a two-step copper catalyzed alkyne-azide cycloaddition (CuAAC) "click" reaction [5]. Moreover, Rodriguez et.al., observed the viability of a DNA sensor based on the facile synthesis of GNRs decorated with Fe<sub>3</sub>O<sub>4</sub> nanoparticles [6]. Zhang et.al., introduced Iron Oxide nano particles into chitosan/graphene based biosensors for multifunctional device applications. It showed that the bio-sensing performance decreased significantly and the linear range was only up to 1.67 mM. The Challenges for introduction of MNP while remaining good performance of chitosan/graphene based biosensors have attracted increasing attention. Improvement of catalytic activity of chitosan/graphene composites via structural modification has been considered as a promising resolution for these issues [7]. Zhong et.al., developed a facile and controllable method for synthesis of Fe<sub>3</sub>O<sub>4</sub> nanoparticles which encapsulated in hollow carbon nanocages (FNHCs) along with SiO<sub>2</sub> nanospheres as a sacrificial template. Owing to the unique structure of multiple Fe<sub>3</sub>O<sub>4</sub> nanoparticles as cores integrated with N-doped carbon nanocages, the results showed that as-synthesized FNHCs exhibited greatly enhanced peroxidase mimicking activity with extremely high signal-to-noise ratio of ~91 fold [8]. Chouhan et.al performed on a new electrochemical sensing device that was constructed for determination of pesticides. In this report, acetylcholinesterase was bioconjugated onto hybrid nanocomposite, i.e. iron oxide nanoparticles and poly (indole-

Tele:

E-mail address: [dhharshinimuthu93@gmail.com](mailto:dhharshinimuthu93@gmail.com)

© 2021 Elixir All rights reserved

5-carboxylic acid) ( $\text{Fe}_3\text{O}_4\text{NPs/Pin5COOH}$ ) was deposited electrochemically on glassy carbon electrode.  $\text{Fe}_3\text{O}_4$  NPs was showed as an amplified sensing interface at lower voltage which makes the sensor more sensitive and specific [9].

It is to be noted that green synthesis in association with nanoscience and technology means the synthesizing of nanomaterials or nanoparticles without using hazardous chemicals that produce toxic by-products. In other words, green method is an eco - friendly technique to synthesize nanoparticles where it is not harmful to the environment and human health. It is true that conventional methods can fabricate nanoparticles in huge quantities with desired morphology and size.

On the other hand, a green synthesized nano particle employs the bottom-up approach where the metal atoms assemble to form clusters and then eventually the nano particles. The compounds present in green based materials may act as both reducing and capping agents that can stabilize the nanoparticles during synthesis process. This may also control the size and shape of the nanoparticles which can be used for various applications.

The present work focuses, *Nyctanthes arbor tristis* that is one of the most useful traditional medicinal plants in India which belongs to the family Oleaceae. The Plant grows in tropical and subtropical region. It is distributed sub Himalayan region of India and also found in Indian gardens as ornamental plant [10]. It is a common wild hardy large shrub or small tree. *N. arbortristis* is commonly known as Night Jasmine, Harsingar and Parijat. Various parts of the plant like seeds, leaves, flowers, bark and fruits have been investigated for their significant pharmacological activity. Phyto Chemicals like flavanoid, glycoside, Organic acids, essential oils, tannic acid, carotene, friedelin, lupeol, glucose, benzoic acid have been reported for significant hair tonic [11]. Hepatoprotective, anti Leishmaniasis, anti viral, anti fungal, anti pyretic, anti histaminic, anti malarial, anti bacterial and anti inflammatory etc., Thus this non toxic and benign seed extract is used for the synthesis of iron oxide nano particles. The literature survey reveals that chemical constituents of *Nyctanthes arbor tristis* seed 3-4 secotriterpene acid, Arbortristoside A & B, glycerides of Linoleic acid, Myristic acids and Nyctanthic acid. The arbortristoside A & B possess immunomodulatory and anti testimonial activities [12 – 13].

Green synthesis of pure and doped  $\text{Fe}_3\text{O}_4$  - NPs are capable to be used in various applications as reported in literature. However, applications of  $\text{Fe}_3\text{O}_4$  - NPs are more concerned by experts nowadays as human health is threaten due to several issues such as pollutions, processed food industry, weather change and unbalance lifestyle. These issues may cause plenty of serious diseases and one of the most popular diseases is cancer.  $\text{Fe}_3\text{O}_4$ -NPs show various applications including antibacterial, tissue engineering and hyperthermia. They also play important roles as magnetic resonance imaging (MRI) contrast agent [14].

By bearing in mind the importance of  $\text{Fe}_2\text{O}_3$  nano particles, the present manuscript focuses the green synthesis of proposed nano particles for super capacitor application using the extraction of *Nyctanthes arbor tristis* for the first time.

## 2. Experimental methods

### Materials and Preparation methods

The precursors such as  $\text{FeCl}_3$  and  $\text{NH}_3$  was purchased from Merc with analytical grade and used as such without any

further purification. The extraction of *Nyctanthes arbortristis* was carried out using deionized water. The mixture of iron solution with the extraction of *Nyctanthes arbortristis* was kept under stirring process in order to obtain pristine iron hydroxide using chemical precipitation method. Further, the supernatant solution was removed and washed several times in order to remove chlorine ions. The obtained powder was dried using hot plate and kept in muffle furnace at  $600^\circ\text{C}/\text{air}/6\text{h}$  in order to remove the impurities and improve the crystallinity.

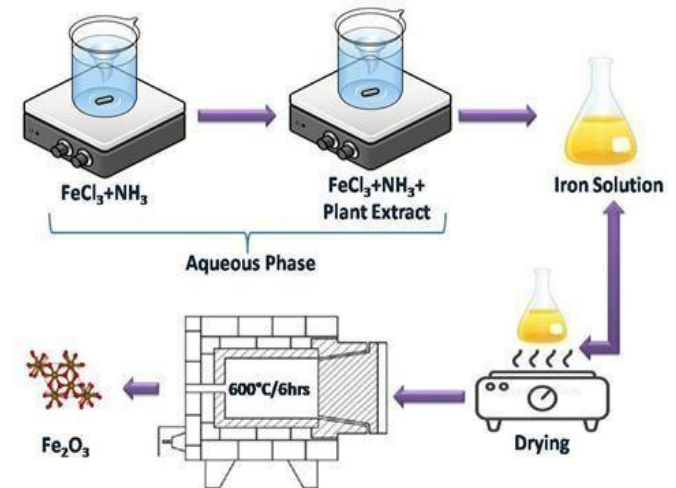


**Figure.1. Schematic representation of the synthesis Process.**

### Characterization methods

The synthesized samples are systematically characterized to study the physico-chemical properties. The structure and crystallinity of the samples are confirmed with BRUKER D8 ADVANCED X-ray Diffractometer in Bragg-Brentano geometry using Cu K-alpha radiation ( $\lambda=1.5406 \text{ \AA}$ ). Surface morphology of the synthesized composite was studied by FE-SEM (HITACHI S-3400). The electrochemical performance of cyclic voltammetry (CV) and charge-discharge technique was carried out by CHI 604C potentiostat in a three electrode assembly.

### 3. Results and Discussion Powder XRD analysis

The respective X-ray diffraction patterns of as prepared and annealed  $\text{Fe}_2\text{O}_3$  nanoparticles are shown in Fig. 2. The diffraction pattern corresponding to as prepared samples showed amorphous in nature reveals the formation of iron hydroxide ( $\text{FeOH}$ ) during synthesis process (Fig. 2a). On the other hand, the diffractogram of annealed  $\text{Fe}_2\text{O}_3$  shows the high intense peak around  $2\theta = 33^\circ.4'$  and the associated peaks at  $35^\circ.4'$  and  $45^\circ.9'$  are corresponding to the planes (104), (110) and (113) belongs to the formation of  $\alpha\text{-Fe}_2\text{O}_3$  with JCPDS card no. – 33 - 0664 [11]. The XRD pattern of  $\alpha\text{-Fe}_2\text{O}_3$  shows a high intensity peaks proves the crystalline nature of the end products. Moreover, the sharpness of the diffraction peaks also indicates the high crystalline nature of  $\alpha\text{-Fe}_2\text{O}_3$  nanomaterials. Furthermore, the diffraction peaks of the nanoparticles are broadened with lower in intensity due to small crystallite size and confirm the presence of  $\alpha\text{-Fe}_2\text{O}_3$  [15]. The corresponding crystallite size in the case of annealed sample calculated from the Debye Scherrer equation was about 30.75 nm. Also, there is no evidence for secondary crystallite phase that attributable to any other oxidation state of Iron, confirms the highly pure  $\alpha\text{-Fe}_2\text{O}_3$  phase in the annealed sample [16].

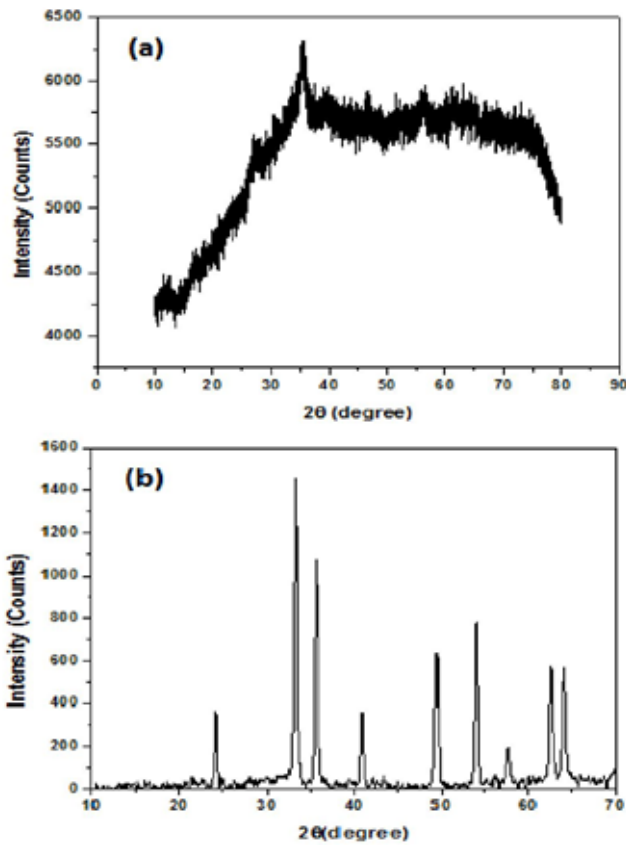


Figure 2. Powder XRD pattern of (a) as prepared (b)  $\alpha$ - $\text{Fe}_2\text{O}_3$  nanoparticles.

#### UV – Visible spectroscopic analysis

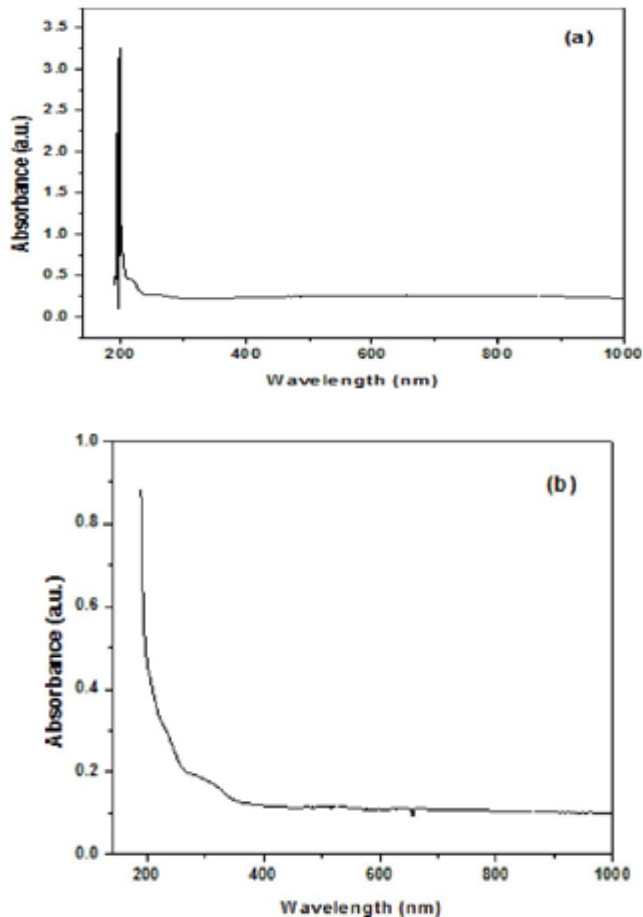


Figure 3. UV Visible absorption spectrum of (a) as prepared (b) annealed Iron oxide ( $\text{Fe}_2\text{O}_3$ ) nanoparticles.

The respective optical properties of the as prepared and annealed ( $\alpha$ - $\text{Fe}_2\text{O}_3$ ) were analyzed using UV-Vis spectroscopic technique. This result indicates that the optical absorption obtained around 363 nm in the case of annealed sample may be attributed to shift towards blue region as shown in Fig.3 and also the obtained absorption edge may be corresponding to  $\alpha$ - $\text{Fe}_2\text{O}_3$  nanoparticles. It is to be noted that the corresponding absorption region arises around 363 nm as prepared and annealed samples which confirmed the shift towards lower wavelength (blue shift) that is in agreement with the powder XRD analysis due to its amorphous and crystalline nature of the prepared materials. In focus, there is no another absorption peaks rose due to the extraction from *Nyctanthesarbortristis*. The values for the as prepared calculated energy band gap and annealed nanoparticles are found to be 3.5 and 5.29 eV respectively using Tauc Plot [17]. It explains the reason for the blue shift of the absorption curve in association with the reduction of the band gap energy and also the recombination rate which may lead to the photovoltaic activity applications of the prepared samples.

#### Microscope analysis

The microscope (FE-SEM) analysis of the prepared samples was analyzed as shown in Fig.4 that explored that the samples were not fully resolved as individual particles due to the formation of as prepared and annealed  $\alpha$ - $\text{Fe}_2\text{O}_3$  due to low calcinations temperature. The morphology of the prepared samples was found to be spherical in nature with the dimension of the order of 2to3  $\mu\text{m}$ . Moreover, the morphology of the samples clearly shows the role of extraction during the synthesis of  $\alpha$ - $\text{Fe}_2\text{O}_3$  nanoparticles in the case of both as prepared and annealed samples [18].

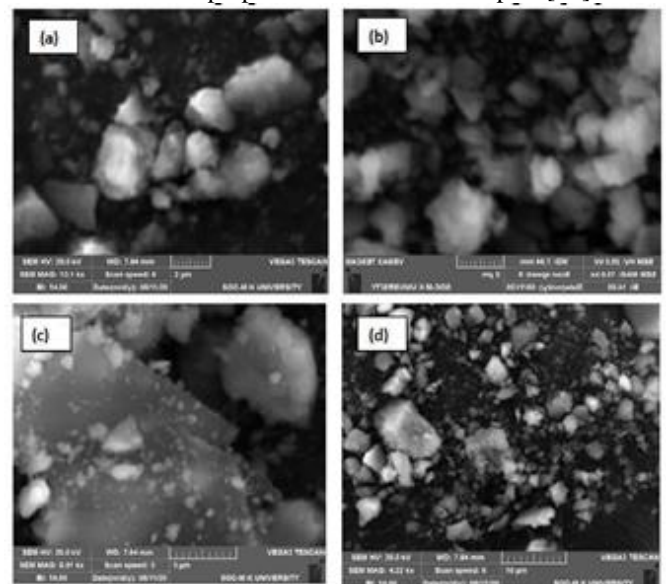


Figure 4. Microscopic images of as prepared (a & b) and annealed Iron oxide (c & d)  $\text{Fe}_2\text{O}_3$  nanoparticles.

#### FT – IR analysis

The corresponding FT-IR spectra which was recorded in the range of 4000-400 $\text{cm}^{-1}$  in ambient condition in the case of annealed sample  $\alpha$ - $\text{Fe}_2\text{O}_3$  nanoparticles is shown in Fig. 5. The FTIR spectra explores the stretching vibrations in the regions between 3175 to 3726  $\text{cm}^{-1}$  belongs to -NH-stretching and alkyl stretching vibrations respectively that confirms the trace of extraction of the plants during synthesis process. Moreover, S = O, C = O and C-S (both stretching and bending vibration) were observed the wavenumber regions around 1628 to 686  $\text{cm}^{-1}$  respectively in order to confirm the functional groups present in the extracted plant of



Nyctanthesarbortristis. In focus, the band around 465 cm<sup>-1</sup> gives the F = O signal which confirms the formation of  $\alpha$ -Fe<sub>2</sub>O<sub>3</sub> nanoparticles and is in agreement with the powder XRD results.

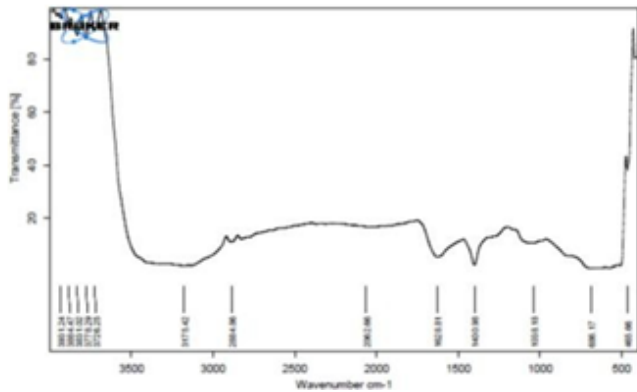


Figure 5. FT-IR spectra for  $\alpha$ -Fe<sub>2</sub>O<sub>3</sub> nanoparticles.

#### BET Surface Area Analysis

The Brunauer-Emmett-Teller (BET) analysis was used to find the effective surface area of the prepared nanomaterials. The results showed that annealed sample (without doping) is having larger surface area (34.46 m<sup>2</sup>.g<sup>-1</sup>) when compared to that of rest of the samples. Also, it is to be noted that the found value is very much higher than that of commercially available Iron oxide nanomaterials (30m<sup>2</sup>.g<sup>-1</sup>) [17]. This occurrence of this large surface area obtained in the case of pure annealed sample may be due to the introduction of efficiencies during the treatment of annealing process of the prepared sample also due to phase transition [18]. Moreover, the contribution of occurring large surface area reflects in the super capacitor applications which is discussed in detail below.

Fe <sub>2</sub> O <sub>3</sub> Nanopowder	
Formation purity	92%
Specific surface area	35 m <sup>2</sup> /g
Nature of morphology	Elongated spherical
Color	Red Brown
Particle size	20 – 40 nm

#### Raman analysis

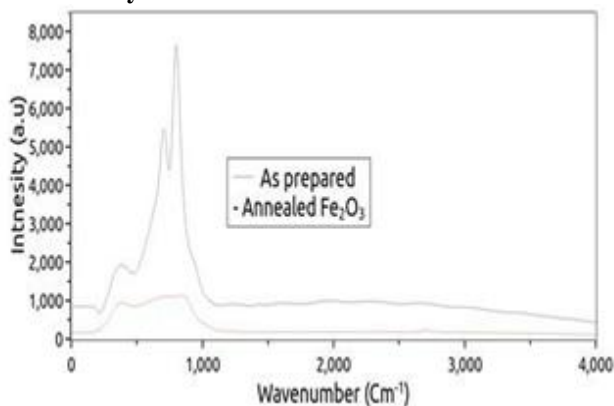


Figure 6. Raman spectrum of as prepared and annealed Fe<sub>2</sub>O<sub>3</sub>.

Figure 6. shows the typical Raman band spectrum in the range 200-1400 cm<sup>-1</sup> in order to confirm the formation of prepared Fe<sub>2</sub>O<sub>3</sub> nanoparticles along with annealed nanomaterials. Raman analysis clearly resembles the trace of Fe-O bending and stretching vibrations between the regions 220-440 cm<sup>-1</sup> and 660-940 cm<sup>-1</sup> respectively. The weak

band peaks observed may be due to less crystalline nature of the prepared materials. On the other hand, in the case of annealed samples there could trace slightly blue-shifted peaks shows the change in degree of crystallinity based on the broadening of respective peaks which may be an another evidence for the formation of Fe<sub>2</sub>O<sub>3</sub> crystalline structure [18].

#### 3.6 Electrochemical analysis

In order find the suitability of the annealed  $\alpha$ -Fe<sub>2</sub>O<sub>3</sub> nanoparticles for supercapacitor applications Cyclic voltammetry study was performed in the voltage window range from 0 to 1 V using three electrodes system in 1 M aqueous solution of FeSO<sub>4</sub>. The corresponding CV curves of the various electrodes recorded with the sweep rates of 10, 20, 40, 60, mVs<sup>-1</sup> at room temperature are illustrated in Fig. 5. The obtained curves due to  $\alpha$ -Fe<sub>2</sub>O<sub>3</sub> nanoparticles shows the excellent capacitive behavior as shown in Fig 4. In focus the lower scan rate the CV curves of the  $\alpha$ -Fe<sub>2</sub>O<sub>3</sub> nanoparticles based electrode exhibit redox peaks attribute to the reversible Faradaic redox reaction at the electrode surface caused by the pseudo-capacitance of the  $\alpha$ -Fe<sub>2</sub>O<sub>3</sub> nanoparticles as an active material, rather than the double layer capacitance. With increase in the scan rate the current response in the composite increases, revealing its favorable capacitive behavior of the prepared  $\alpha$ -Fe<sub>2</sub>O<sub>3</sub> nanoparticles. Also the nature clearly represents the linear progress CV curves at the high scan rates with the current response to voltage reverse at each potential.

The very low equivalent series resistance of the electrode and rapid diffusion of electrolyte ions in  $\alpha$ -Fe<sub>2</sub>O<sub>3</sub> nanoparticles are confirmed by nearly straight side of the square shaped curves also in rectangular.

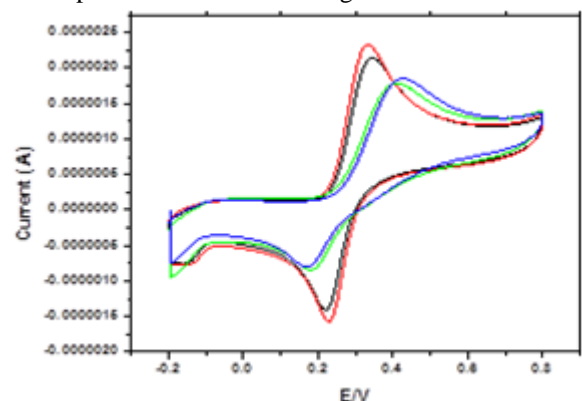


Figure 7. Electrochemical performance of as prepared and annealed Iron oxide (Fe<sub>2</sub>O<sub>3</sub>) nanoparticles.

#### 4. Conclusions

An Eco friendly  $\alpha$ -Fe<sub>2</sub>O<sub>3</sub> nanoparticles and cost-effective approach has been developed at room temperature for the first time. The powder XRD analysis revealed the Crystalline also clustered  $\alpha$ -Fe<sub>2</sub>O<sub>3</sub> nanoparticles with 2–3  $\mu$ m size are observed in the Powder XRD analysis as well as in microscopic analysis. The Raman spectra and corresponding BET analysis clearly evidenced the contribution of annealing process in order to improve the efficiency of the prepared Fe<sub>2</sub>O<sub>3</sub> nanomaterials. The resulting electrochemical activities of  $\alpha$ -Fe<sub>2</sub>O<sub>3</sub> nanoparticles with a large specific capacitance at a scan rate of 1 Ag<sup>-1</sup>, which is found to be greater than that of as prepared  $\alpha$ -Fe<sub>2</sub>O<sub>3</sub> nanoparticles. It is due to the fact that it provides electrical and ionic conducting channels in an electrolyte which plays major role for the high capacitance value. Hence, this present work demonstrates a novel idea and design for a high performance Supercapacitor  $\alpha$ -Fe<sub>2</sub>O<sub>3</sub>

based nanoparticles by a simple and low-temperature synthesis process.

## 5. References

- [1] A. Ali, M. S. AlSalhi, M. Atif, Anees A. Ansari, Muhammad Qadir Israr, J. R. Sadaf, E. Ahmed, Omer Nur and Magnus Willander 2013 *Potentiometric urea biosensor utilizing nanobiocomposite of chitosan-iron oxide magnetic nanoparticles* Conference Series 414.
- [2] Kang Li, Yanjun Lai, Wen Zhang, Litong Jin 2011 *Fe<sub>2</sub>O<sub>3</sub> @ Au core/shell nanoparticle-based electrochemical DNA biosensor for Escherichia coli detection* 84 607.
- [3] Mokhtar Hjiri, Mohamed Salah Aida, Giovanni Neri *NO<sub>2</sub> selective sensor based on  $\alpha$ -Fe<sub>2</sub>O<sub>3</sub> nanoparticles synthesized via hydrothermal technique* *Sensors* 2019, **19**(1), 167.
- [4] Ming-Yan Wang, Tao Shen, Meng Wang, Dong-En Zhang, Zhi-wei Tong, Jun Chen 2013 *One-pot synthesis of  $\alpha$ -Fe<sub>2</sub>O<sub>3</sub> nanoparticles-decorated reduced graphene oxide for efficient non enzymatic H<sub>2</sub>O<sub>2</sub> biosensor* <http://dx.doi.org/10.1016/j.snb.2013.08.091>.
- [5] Mahesh K.P.O, Indrajit Shown, Li-Chyong Chen, Kuei-Hsien Chen, Yian Tai 2018 *Flexible sensor for dopamine detection fabricated by the direct growth of  $\alpha$ -Fe<sub>2</sub>O<sub>3</sub> nanoparticles on carbon cloth* 427 387.
- [6] Xinha Shi, Wei Gu, Bingyu Li, Ningning Chen, Kai Zhao & Yuezhong Xian 2014 *Enzymatic biosensors based on the use of metal oxide nanoparticles* 181 doi:10.1007/00604-013-1069-5.
- [7] Bansal Gulshan, Suri KA, Grover Parul 2015 *A Comprehensive review on Nyctanthes arbortristis* 7 0975.
- [8] Hetal Bhalakiya, Nainesh R. Modi 2019 *Traditional medicinal uses, phytochemical profile and pharmacological activities of nyctanthes arbortristis*. doi:10.26479/2019.0502.76 .
- [9] Sathish Kumar Ponnaiah, Prakash Periakaruppan, and Balakumar Vellaichamy 2018 *A new electrochemical sensor based on silver doped iron oxide nanocomposite coupled with polyaniline and its sensing application for picomolar level detection of uric acid in human blood and urine samples* doi: 10.1021/acs.jpcc.7b11504.
- [10] M W Akram, M F Alam, H N Ji, A Mahmood, Tariq Munir, M Z Iqbal, M R Saleem, N.Amin and A G Wu 2019 *IOP Conf. Series: Materials Science and Engineering* 474 012060.
- [11] Saurabh Kumar, Mohammad Umar, Anas Saifi, Suveen Kumar, Shine Augustine, Saurabh Srivastava, Banshi D. Malhotra 2019 *Electrochemical paper based cancer biosensor using iron oxide nanoparticles decorated PEDOT:PSS* 135 1056.
- [12] R. M. Kershi, F. M. Ali, M. A. Sayed 2018 *Journal of Advanced Ceramics* 7(3) 218 <https://doi.org/10.1007/s40145-018-0273-5>.
- [13] Nirmal Prabhakar, Himkusha Thakur, Anu Bharti, Navpreet Kaur 2016 *Chitosan-iron oxide nanocomposite based electrochemical aptasensor for determination of Malathion* doi: 10.1016/j.aca.2016.08.015.
- [14] Mustafa Aghazadeh, Isa Karimzadeh, Mohammad Reza Ganjali, Mohammad Ghannadi Maragheh 2017 *Journal of Materials Science: Materials in Electronics* <https://doi.org/10.1007/s10854-017-8481-2>.
- [15] R D Widodo1 , Priyono, Rusiyanto, S Anis, A A Ichwani, B Setiawan, D F Fitriyana, L Rochman 2020 *Synthesis and characterization of iron (III) oxide from natural iron sand of the south coastal area Purworejo Central Java* *Journal of Physics: Conference Series* 1444 012043
- [16] Xu, Siyang & Habib, Ashfaq & Gee, Sung-Hoon & Hong, Y. & McHenry, Michael 2015 *Spin orientation, structure, morphology, and magnetic properties of hematite nanoparticles* *Journal of Applied Physics* 117. 17A315. 10.1063/1.4914059
- [17] Simone Piccinin 2019 *The band structure and optical absorption of hematite ( $\alpha$ -Fe<sub>2</sub>O<sub>3</sub>): a first-principles GW-BSE study* *Phys. Chem. Chem. Phys.*, 21 2957
- [18] G Gnanaprakash 2006 *Magnetic nanoparticles with enhanced  $\gamma$ -Fe<sub>2</sub>O<sub>3</sub> to  $\alpha$ -Fe<sub>2</sub>O<sub>3</sub> phase transition temperature* *Nanotechnology* 17 5851.